Cancer Immunol Immunother (2008) 57:1879–1890
DOI 10.1007/s00262-008-0518-1

ORIGINAL ARTICLE

Kinetics of anti-carcinoembryonic antigen antibody internalization: effects of affinity, bivalency, and stability

Michael M. Schmidt · Greg M. Thurber · K. Dane Wittrup

Received: 25 November 2007 / Accepted: 31 March 2008 / Published online: 12 April 2008

Abstract Theoretical analyses suggest that the cellular internalization and catabolism of bound antibodies contribute significantly to poor penetration into tumors. Here we quantitatively assess the internalization of antibodies and antibody fragments against the commonly targeted antigen carcinoembryonic antigen (CEA). Although CEA is often referred to as a non-internalizing or shed antigen, anti-CEA antibodies and antibody fragments are shown to be slowly endocytosed by LS174T cells with a half-time of 10–16 h, a time scale consistent with the metabolic turnover rate of CEA in the absence of antibody. Anti-CEA single chain variable fragments (scFvs) with significant differences in affinity, stability against protease digestion, and valency exhibit similar uptake rates of bound antibody. In contrast, one anti-CEA IgG exhibits unique binding and trafficking properties with twice as many molecules bound per cell at saturation and significantly faster cellular internalization after binding. The internalization rates measured herein can be used in simple computational models to predict the microdistribution of these antibodies in tumor spheroids.

Keywords Tumor targeting · CEA · Endocytosis · Antibody fragments · Affinity

Electronic supplementary material The online version of this article (doi:10.1007/s00262-008-0518-1) contains supplementary material, which is available to authorized users.

M. M. Schmidt · K. D. Wittrup (✉)
Department of Biological Engineering,
Massachusetts Institute of Technology, Building E19-551,
50 Ames Street, Cambridge, MA 02139, USA
e-mail: wittrup@mit.edu

G. M. Thurber · K. D. Wittrup
Department of Chemical Engineering,
Massachusetts Institute of Technology, Building E19-551,
50 Ames Street, Cambridge, MA 02139, USA

Introduction

Antibody drugs have begun to show clinical promise for the treatment of a variety of cancers—there are currently nine FDA approved antibodies for cancer treatment with dozens more in clinical trials [3]. By specifically targeting antigens overexpressed on tumor cells, these drugs have potential to improve the efficacy of cancer treatment while limiting toxic exposure to healthy cells. Despite this progress, there are still significant barriers that must be overcome in order for these drugs to reach their full potential. In particular, efficacy has been limited in the treatment of solid tumors [6]. The reasons for incomplete cell killing in solid tumors are complex, but one significant factor is that antibodies often fail to fully penetrate the tumor tissue leaving regions of untargeted, viable cancer cells [6].

The transport of antibodies into solid tumors is a complex process involving circulation and clearance from the plasma, extravasation across capillary walls, binding and diffusion in the tumor interstitium, and internalization and catabolism in tumor cells. Solid tumors typically exhibit abnormal physiology characterized by high interstitial fluid pressure, insufficient vascularization, and dense extracellular matrix that limit antibody movement [21]. After entering the tumor, high affinity antibodies rapidly bind to free antigen depleting the pool of free antibody and further hindering penetration [2, 16, 18]. Recent theoretical analyses have suggested that antibody internalization and catabolism in tumor cells may also contribute to poor antibody transport [37]. Specifically, the time scale model derived by Thurber et al. predicts that incomplete antibody penetration

will occur if the rate of antibody catabolism is faster than the rate of antibody extravasation and diffusion. The antibody internalization rate has also been predicted to influence the length of antibody retention in the tumor, surface accessibility of antibody for ADCC or pretargeted radioimmunotherapy, and the cytotoxicity of immunotoxins and antibody–drug conjugates [5, 35, 39]. In order to test these predictions, it is imperative to measure accurate rate constants for antibody uptake in tumor cells, which can vary widely for different antigen targets [1, 4]. Additionally, it is important to understand how antibody properties such as affinity, valency, and stability influence these rates, in order to select agents with suitable properties for a given targeting application.

Carcinoembryonic antigen (CEA) is a 180 kDa GPI-linked cell-surface glycoprotein normally expressed in the fetal gut and on the lumenal surface of the adult colon [19]. During colorectal carcinoma oncogenesis, CEA loses its polarity and becomes overexpressed throughout the tumor tissue. High levels of CEA expression have also been observed in epithelial tumors in the lung, breast, thyroid, and ovaries [19]. Due to this selective tumor overexpression, antibodies against CEA have been investigated as targeting agents for a number of imaging and therapeutic approaches including SPECT and PET imaging, pretargeted radioimmunotherapy, and ADEPT [9, 22, 32, 38].

Although CEA is often referred to as a shed or non-internalizing antigen [7, 8, 25], there have been sporadic reports that antibodies and immunoconjugates against CEA are in fact slowly internalized by CEA expressing tumor cells [14, 33, 34]. However, these studies have lacked: (1) quantitative measurement of the bound antibody internalization rate constant (k_e) and (2) systematic study of how antibody properties such as affinity, stability, and valency influence this uptake. These limitations are addressed in the current study in which the internalization rates of a series of anti-CEA antibodies and antibody fragments with differences in affinity, stability to protease degradation, valency, and target epitope have been quantitatively measured in CEA expressing cell lines.

Materials and methods

Materials and cell lines

Anti-CEA IgGs M85151a and M111147 were purchased from Fitzgerald (Concord, MA). LS174T cells were obtained from ATCC (Rockville, MD). LIM1215 and SW-1222 cells were the kind gift of the Ludwig Institute. Cells were grown in minimum essential media (MEM) supplemented with 10% FBS and 1% penicillin–streptomyocin. CEA expressing HT-1080 cells (HT-1080-CEA) were created by transfecting HT-1080 cells with the pIRES-CEA plasmid (kind gift of Dr. G. Prud'homme, St. Michael's Hospital, Toronto, Canada) using lipofectamine according to manufacturer's instructions. Transfected cells were selected by growth for 7 days in MEM with 0.75 mg/mL G418.

Antibody fragment production

Secretion vectors for shMFE and sm3E containing a C-terminal His_6 tag have been described previously [17]. Disulfide stabilized scFvs were produced by mutating residues R44 and G234 to cysteine using the QuikChange Kit (Stratagene) according to manufacturer's instructions. Mutations were confirmed by sequencing. Plasmids were transformed into the YVH10 strain of yeast using the EZ Yeast Kit (Zymo Research) and plated on SD-CAA media supplemented with 40 μg/mL tryptophan. Individual colonies were grown in 1 L flasks and secretion induced for 48 h at 37°C as described previously [17]. The cleared supernatant was concentrated using Millipore 10 kDa ultrafiltration membranes and the His-tagged proteins purified using BD Talon metal affinity resin following the manufacturer's batch-column protocol. Eluted proteins were further purified by anion exchange chromatography on a Hi-Q column equilibrated with 20 mM Tris buffer at pH 8.25 and size exclusion chromatography on a Superdex 75 column (GE Healthcare). Samples were run on a 12% Bis–Tris gel with or without 100 mM DTT and Coomassie stained to check size and purity. Fab fragments were produced from IgG M85151a by papain digestion using the ImmunoPure Fab Preparation Kit (Pierce) according to manufacturer's instructions. Purified antibody fragments were conjugated to Alexa-488 fluorophores using the Microscale Protein Labeling Kit (Invitrogen) following manufacturer's instructions. Protein concentration and degree of fluorophore labeling were determined from UV absorbance at 280 and 490 nm as described in the Microscale Kit. The immunoreactive fraction was estimated by incubating scFvs with a fivefold molar excess of soluble CEA (Fitzgerald) and determining the fraction of antibody that elutes as a complex on size exclusion chromatography.

Linker cleavage and protease stability

The $(Gly_4Ser)_3$ linker connecting the V_H and V_L domains of the scFvs was cleaved by incubating the antibody fragments with 0.02 units/mL subtilisin in digestion buffer (20 mM Tris–HCl, 5 mM calcium chlorate, pH 7.5) for 90 min at 37°C. Digested samples were run on a 12% Bis–Tris gel with or without 100 mM DTT and Coomassie stained. For functional protease stability assays, Alexa-488 labeled scFvs were incubated with increasing

concentrations of subtilisin in digestion buffer for 60 min at 37°C. Trypsinized LS174T cells were labeled with the digested antibody fragments at subsaturating concentrations for 20 min on ice and mean cellular fluorescence measured on an EPICS Coulter XL flow cytometer (Beckman Coulter, Inc.)

Cell–surface binding

Trypsinized LS174T cells were fixed with Cytofix Buffer (BD Biosciences) for 20 min at 4°C to prevent antibody trafficking. For K_D measurements, fixed cells were incubated with Alexa-488 labeled antibodies or antibody fragments at a range of concentrations for 16–20 h at 37°C. To avoid antibody depletion effects, a tenfold molar excess of antibody over antigen was maintained throughout. Labeled cells were washed twice with PBS + 0.1% BSA, and the mean Alexa-488 cellular fluorescence measured on an EPICS Coulter XL cytometer. The normalized signal was fit to the equation MFU = B_{max} ([Ab]/([Ab] + K_D)) to determine the K_D. For k_{off} measurements, fixed cells were labeled overnight with saturating concentrations of Alexa-488 conjugated scFvs. Cells were washed and resuspended at 37°C in PBS–BSA containing 100 nM unlabeled sm3E to prevent rebinding of dissociated antibodies. At each time point, cells were washed and the mean fluorescence quantified by flow cytometry. Fluorescence values were normalized by the signal at $t = 0$ and fit to an exponential decay to determine the k_{off}. The number of antibodies bound per cell at saturation was determined by labeling cells with saturating concentrations of Alexa-488 conjugated antibodies or antibody fragments and converting the fluorescence intensity to a number of molecules using Alexa-488 calibration beads and the calculated number of fluorophores per antibody.

Net antibody internalization assays

LS174T cells were subcultured into 96-well plates at a concentration of 10^5 cells per well and allowed to adhere for 12–16 h. After washing cells once in media, 125 μL of Alexa-488 conjugated antibodies or antibody fragments at a concentration of 20 nM in MEM + FBS was added to each well. Cells were incubated at 37°C in the continuous presence of the labeled antibodies. At each time point, plates were chilled, wells washed twice in PBS–BSA, and cells lifted by incubating with 200 μL cell dissociation buffer (Gibco) for 10 min on ice. Dissociated cells were transferred to microfuge tubes by pipetting and sedimented at 14,000×g. Cell pellets were resuspended in PBS–BSA with or without 25 μg/mL anti-Alexa-488 quenching IgG (molecular probes) for 25 min on ice. The mean fluorescence of the surface quenched and unquenched cells was measured on an XL cytometer and used to calculate the relative amounts of surface and internal fluorescence as described previously [4]. In brief, surface fluorescence was determined as (unquenched MFU − quenched MFU)/ε, where ε is the quenching efficiency determined by comparing the quenched and unquenched signals of cells that had been labeled briefly on ice to prevent internalization. The internal fluorescence was then calculated as total MFU − surface MFU. Non-specific internalization of antibodies due to fluid phase uptake was measured using cells where the CEA was pre-blocked with unlabeled antibody and subtracted from the internal signal. The corrected internal MFU values were plotted against the integral of the surface fluorescence determined using the trapezoidal rule and fit to a linear curve, the slope of which is the internalization rate k_e [26]. scFv uptake experiments in the LIM1215, SW-12222, and HT-1080-CEA cell lines were performed essentially as described above except trypsin–EDTA was used in place of cell dissociation buffer to lift the cells from the plates at each time point.

Surface decay

LS174T cells subcultured in 96-well plates as above were surface labeled with saturating concentrations of Alexa-488 labeled sm3E, ds-shMFE-M, or M85151a IgG for 1 h on ice. Unbound antibody was washed from each well and cells were incubated in media at 37°C. At each time point, cells were chilled and transferred to microfuge tubes as described above. Cells were then surface labeled on ice with PE conjugated secondary and tertiary antibodies to determine the amount of anti-CEA antibody remaining on the surface. Goat anti-mouse PE (1:50 dilution) was used for M85151a and anti-His biotin (1:70 dilution) followed by streptavidin-PE (1:100 dilution) for the scFvs. Cells were analyzed by flow cytometry to measure the 488 signal (total cell-associated antibody) and PE signal (surface accessible antibody). Cells were also imaged for 488 and PE colocalization using a Deltavision deconvolution microscope (Applied Precision, Inc.)

Fluorescence imaging

LS174T cells were subcultured at ~2 × 10^5 cells per well on 8-well glass coverslip bottom dishes (Nunc). After attachment, cells were incubated overnight at 37°C with 10 nM anti-CEA scFvs conjugated to either Alexa-488 or Alexa-594. Cells were then labeled for 1 h at 37°C with fluorescent markers of endocytosis including 1 μg/mL Cholera toxin subunit B-594, 20 μg/mL transferrin-488, 10 μM dextran-488, or 100 nM LysoTracker red. Cells were washed and imaged on a Deltavision deconvolution microscope to determine 488 and 594 colocalization.

CEA downregulation

LS174T cells subcultured into 96-well plates as above were incubated at 37°C in media with or without 50 nM unlabeled anti-CEA antibodies or antibody fragments. At each time point, cells were chilled, washed twice with cold CO_2 independent media, and labeled for 40 min on ice with 20 nM of a non-competitive Alexa-488 labeled anti-CEA antibody. Cells were then washed, lifted with cell dissociation buffer, and analyzed by flow cytometry as above. The Alexa-488 signal of cells incubated with unlabeled antibody was normalized by the signal of cells incubated with media alone to determine the degree of antigen downregulation.

Biotinylated CEA turnover

LS174T cells were subcultured into 12-well plates at a density of 2×10^6 cells per well and grown for 24 h at 37°C. Cells were washed and surface biotinylated with 1 mg/mL NHS-SS-biotin (Pierce) in PBS, pH 8.0. The labeling reaction was quenched after 30 min by the addition of 100 mM Tris–HCl. The cells were then washed twice in media and incubated at 37°C. At each time point, cells were placed on ice, washed twice with PBS–BSA, and incubated in 500 μL of ice cold lysis buffer for 10 min. The cell lysate was cleared by centrifuging at 14,000×*g* for 15 min and biotinylated proteins pulled down with streptavidin resin (Pierce). The bound proteins were washed and eluted by cleaving the disulfide linker with 100 mM DTT. Eluted samples were run on a 4–12% SDS-PAGE gel, transferred to a nitrocellulose membrane, and blotted for CEA using M85151a IgG (1:1,000 dilution) and goat anti-mouse-HRP secondary (1:1,000 dilution). Band intensities at each time point were quantified using QuantityOne Software (Bio-Rad) and normalized by the band intensity at time zero.

Results

The internalization rate of cell bound antibodies and antibody fragments is predicted to significantly alter the microdistribution, surface accessibility, and retention time of these molecules in tumor tissue. Therefore, we set out to quantitatively measure the internalization of antibodies and antibody fragments directed against the common tumor target CEA. Furthermore, we examined how antibody parameters such as affinity, stability to protease digestion, valency, and target epitope influence these internalization rates.

scFv production

As a model system to examine the effect of antibody properties on cellular uptake, we developed a series of anti-CEA single-chain variable fragments (scFvs) with differences in affinity, stability to protease degradation, and valency. scFvs are ~27 kDa antibody fragments consisting of the V_H and V_L domains of an IgG connected by a peptide linker. Previous affinity maturation work resulted in two scFvs sm3E and shMFE that bind to the same epitope on CEA with a nearly 300-fold difference in affinity (sm3E K_D = 30 pM, shMFE K_D = 8.5 nM) [17]. To make fragments with increased stability, cysteine residues were inserted into the V_H and V_L domains of the proteins to form an interdomain disulfide bond. The formation of this interdomain disulfide has been shown to increase the protease and thermal stability of antibody fragments [11, 31]. Additionally, the disulfide stabilized scFvs (ds-scFvs) are secreted in yeast as a mix of disulfide locked monomers (ds-scFv-M) and dimers (ds-scFv-D) which can be separated to provide fragments with differences in valency.

Secreted antibody fragments were concentrated and purified at a final yield of 0.5–1 mg/L. All proteins matched expected sizes when run on non-reducing and reducing SDS-PAGE and demonstrated purity greater than 99% (Fig. 1a, b). The slightly increased mobility of the disulfide stabilized monomers compared to the native scFvs under non-reducing conditions is indicative of interdomain disulfide bond formation, which produces a more compact denatured structure. Formation of the interdomain disulfide was further confirmed by proteolytically cleaving the peptide linker connecting the V_H and V_L domains of the scFvs and assaying protein mobility on SDS-PAGE. Following linker cleavage, the V_H and V_L domains of the disulfide stabilized scFvs are held together under non-reducing conditions by the interdomain disulfide bond (Fig. 1c).

scFv binding and stability

Antibody affinity and avidity was assessed by measuring the binding of Alexa-488 conjugated antibody fragments to fixed LS174T cells (Table 1). Both disulfide locked monomers exhibit dissociation constants (30 pM for ds-sm3E-M and 9.2 nM for ds-shMFE-M) similar to those measured previously for sm3E and shMFE by yeast surface display [17]. In contrast, the bivalent molecule ds-shMFE-D has roughly a 100-fold higher apparent affinity (85 pM) than its monomeric counterpart due to avidity from bivalently binding to cells. Interestingly, the non-disulfide stabilized shMFE also exhibits a higher affinity than ds-shMFE-M, likely due to the formation of non-covalent dimers in solution. The formation of such reversible dimers has been observed previously for a closely related scFv MFE-23 [24]. sm3E and ds-sm3E-D demonstrate less significant increases in apparent affinity compared to their monomeric counterpart ds-sm3E-M, although this is likely due to the high affinity of the monovalent interaction rather than an

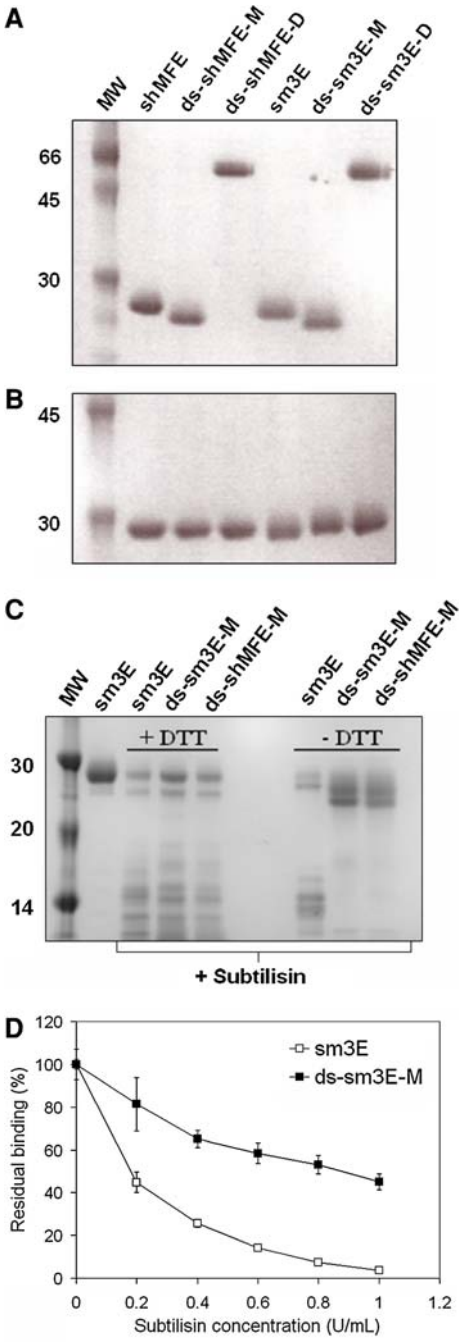

Fig. 1 Production and characterization of anti-CEA scFvs. **a**, **b** SDS-PAGE analysis of scFvs under non-reducing (**a**) and reducing (**b**) conditions. Purified scFvs were run on a 12% Bis–Tris gel with or without 100 mM DTT. All antibody fragments run at their expected molecular weights and are ~99% pure. **c** Cleavage of interdomain linker confirms that interdomain disulfide bond is formed in ds-scFvs. The peptide linker connecting the V_H and V_L domains of each scFv was cleaved with low concentrations of subtilisin, and samples were analyzed by SDS-PAGE. Following linker cleavage, the native scFvs run as 14 kDa proteins on a non-reducing SDS-PAGE gel indicative of separate V_H and V_L domains, while the disulfide stabilized fragments run as 27 kDa proteins as the interdomain disulfide holds the V_H and V_L together. In the presence of DTT, the interdomain disulfide is reduced and the digested ds-scFvs run as separate V_H and V_L domains. **d** Interdomain disulfide bond increases functional protease stability of ds-scFvs. Alexa-488 labeled anti-CEA scFvs with or without the interdomain disulfide bond were incubated with increasing concentration of subtilisin and used to label fixed LS174T cells at subsaturating concentrations. The disulfide stabilized fragment maintains significantly greater binding activity following protease treatment

Table 1 Binding to fixed LS174T cells

scFv	K_D (pM)	$k_{off\ compet}$ (min^{-1})	$t_{1/2\ off\ compet}$
sm3E	26 ± 4	7.5×10^{-5}	153.8 h
ds-sm3E-M	30 ± 5	2.4×10^{-4}	48.1 h
ds-sm3E-D	9.6 ± 0.7	9.6×10^{-5}	120.1 h
shMFE	160 ± 24	6.6×10^{-2}	10.5 min
ds-shMFE-M	9,300 ± 3,300	1.6×10^{-1}	4.3 min
ds-shMFE-D	85 ± 5	8.0×10^{-2}	8.7 min

absence of bivalent binding. Off-rate measurements in the presence of unlabeled competitor support the conclusion that both disulfide stabilized dimers and native scFvs bind to the cell bivalently as their dissociation constants were ~2–3-fold slower than those of the disulfide locked monomers (Table 1). In the absence of competitor, dissociation rates for these bivalent antibody fragments would be significantly slower due to continued rebinding of the two arms [27]. The high affinity scFvs were also >95% functional as determined by soluble CEA binding assays as described in "Materials and methods" (data not shown).

The contribution of the interdomain disulfide to functional scFv stability was assessed by incubating the antibody fragments in increasing concentrations of the protease subtilisin, then measuring binding to LS174T cells at subsaturating concentrations. As expected, the disulfide stabilized proteins displayed significantly higher binding activity following protease treatment than the native scFvs suggesting improved stability (Fig. 1d). As a whole, the in vitro cell binding assays confirmed that the secreted scFvs exhibited the expected differences in affinity, stability to protease digestion, and valency, and were therefore a useful model system for the effects of variation in these parameters on net internalization.

Internalization rate constant (k_e) measurements

The cellular net internalization rate constant (k_e) of each scFv was assayed using a fluorescence quenching protocol, similar to the one described previously for Herceptin endocytic trafficking [4]. Adherent LS174T cells were incubated at 37°C in the continuous presence of Alexa-488 labeled antibody fragments. At each time point, cells were chilled, lifted, and half of the cells surface quenched with anti-Alexa-488 IgG. The efficiency of surface quenching was independently measured for each antibody fragment using

cells that had been labeled briefly on ice to prevent internalization, and ranged from 84 to 91%. The fluorescence intensity of quenched and unquenched samples was quantified by flow cytometry and the surface and internal fluorescence calculated as described in "Materials and methods". In general, the surface fluorescence increases over the first hour and then plateaus as antibody binding reaches equilibrium, while the internal fluorescence continues to increase over time as antibodies are endocytosed and the fluorophores retained in the cell (Fig. 2a). Unlike fluorescein, Alexa-488 fluorescence is not quenched at intracellular pH so there is no significant decrease in signal intensity of endocytosed fluorophores. Non-specific uptake was measured using cells that had been pre-blocked with unlabeled sm3E and was generally found to be low at the experimental antibody concentrations.

Internalization rates were derived from the quenched fluorescence data by plotting the internal fluorescence against the time integral of the surface fluorescence and applying a linear fit (Fig. 2b and Supplemental Fig. 1). Uptake rates were measured in this manner for all scFvs and are reported as internalization half-times in Fig. 2c (where $t_{1/2} = \ln(2)/k_e$). In general, internalization of the anti-CEA scFvs is slow with half-times ranging from 10 to 16 h. Surprisingly, neither antibody affinity, stability to protease digestion, nor valency significantly affect the internalization rate of bound antibody

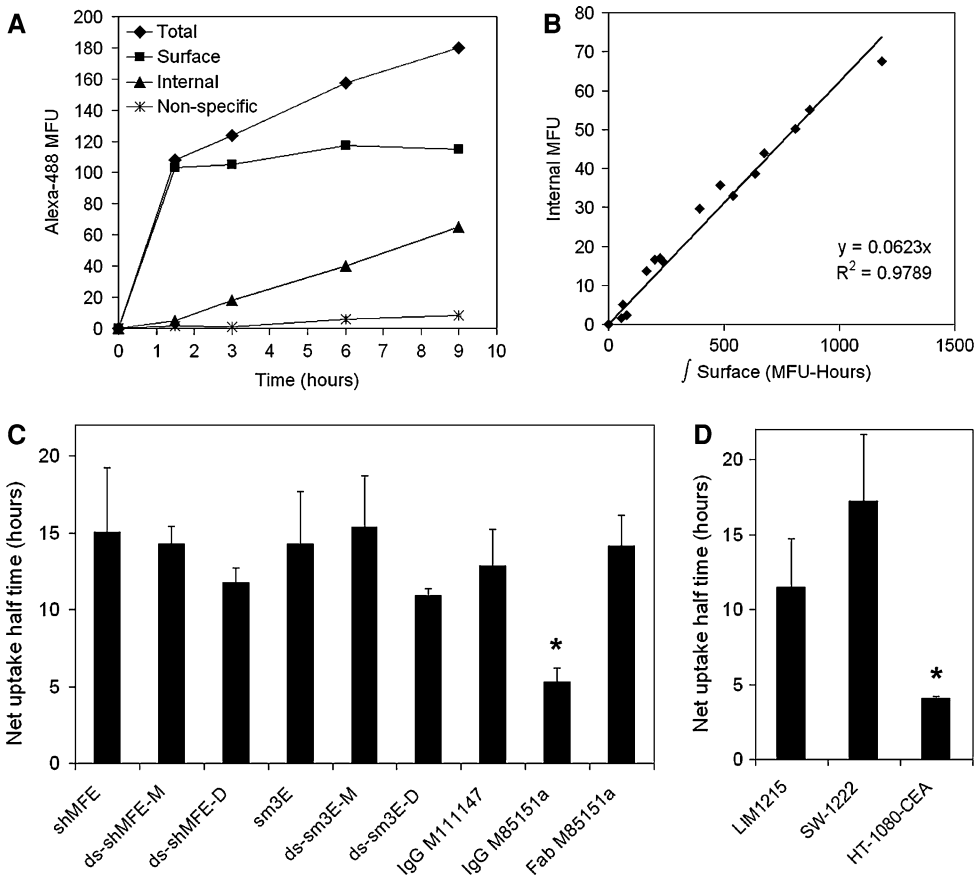

Fig. 2 Net cellular uptake rates of anti-CEA antibodies. **a** Surface quenching allows for distinction of surface and internal antibody fractions. LS174T cells were continuously incubated at 37°C in the presence of Alexa-488 labeled antibodies. Total cellular fluorescence was measured at each time point by flow cytometry and the internal and surface fractions determined by surface quenching with an anti-Alexa-488 IgG as described in "Materials and methods". Non-specific uptake was measured by pre-blocking CEA with a 100-fold excess of unlabeled antibody and was generally low. Data pictured is for an individual experiment with ds-sm3E-D. **b** Derivation of internalization rate k_e. Internal fluorescence values measured as in **a** are plotted against the integral of the surface fluorescence determined by the trapezoidal rule and fit to a linear curve. The slope of the linear fit is the internalization rate k_e. Data points pictured are pooled from four separate experiments with ds-sm3E-D. **c** Anti-CEA antibodies are generally internalized on a 10–16 h time scale. Internalization rates were determined for all antibodies and plotted as a half-time for antibody net uptake. With the exception of IgG M85151a, all tested antibodies are internalized slowly with a half time of 10–16 h. IgG M85151a is internalized significantly faster with a half-time of ~5 h ($^*p < 0.001$). Half-times are the average of three to six individual experiments for each antibody and error bars are SD. **d** CEA expressing HT-1080 cells rapidly internalize ds-sm3E-M. Cellular internalization rates of Alexa-488 labeled ds-sm3E-M were determined in multiple CEA expressing cell types using the fluorescence quenching protocol described above. Colon carcinoma lines LIM1215 and SW-1222 internalize the scFv at similar rates as LS174T, while HT-1080 fibrosarcoma cells transfected with a CEA expression plasmid internalize the antibody fragment more rapidly

fragments in this assay as there is no significant difference in uptake half-times among the scFvs.

The fluorescence quenching protocol was also used to measure the uptake rates of a pair of commercially available anti-CEA IgGs M111147 and M85151a. These antibodies bind to different (non-competing) epitopes on CEA from the scFvs and each other (data not shown) and have functional affinities of 70 pM for M111147 and 7 pM for M85151a as measured by cell surface titration. While M111147 was internalized with a half-time of 13 h, similar to the scFvs, M85151a was taken up significantly faster with a half-time of 5 h (Fig. 2c). A monovalent Fab fragment of M85151a with a functional affinity of 2.5 nM was internalized with a net uptake rate ($t_{1/2} \sim 14$ h) significantly slower than the IgG, suggesting that the bivalency of the full antibody is necessary for its faster uptake (Fig. 2c).

The effect of cell type on anti-CEA antibody fragment internalization was assessed by measuring the internalization of the high affinity scFv ds-sm3E-M in three additional cell lines. LIM1215 and SW-1222 are colon carcinoma cell lines that express CEA at lower levels than LS174T, while HT-1080-CEA is a fibrosarcoma cell line transfected with a CEA expression plasmid resulting in antigen overexpression. LIM1215 and SW-1222 internalized ds-sm3E-M with half-times of 11.5 and 17.2 h, respectively, both similar to the 15.3 h half-time measured in LS174T cells (Fig. 2d). In contrast, HT-1080-CEA cells internalized the scFv at a significantly faster rate with a net uptake half-time of 4 h.

Antibody surface decay

Antibody internalization was also measured in the context of a pulse labeling experiment that better simulates the retention phase of tumor targeting. LS174T cells were surface labeled on ice with Alexa-488 conjugated anti-CEA scFvs or IgG, washed to remove unbound molecules, and incubated at 37°C. At each time point, cells were surface labeled on ice with PE-conjugated anti-mouse or anti-His_6 secondary antibodies, and the 488 and PE signals measured by flow cytometry to determine the total cell associated and surface antibody, respectively. The high affinity scFv sm3E exhibits slow decay of both the total antibody and surface accessible fluorescence (Fig. 3a). The decrease in total signal may be due to antibody dissociation, antigen shedding, or cellular efflux of degraded fluorophore. The surface signal drops faster than the total signal over the course of several hours, indicating a slow internalization of scFv in rough agreement with the k_e values measured in the continuous uptake experiments. In contrast to sm3E, the surface level of M85151a IgG drops rapidly over the first 3 h to approximately 50% of its initial level while the total signal remains virtually unchanged, suggesting a more rapid internalization as observed in the continuous uptake experiments (Fig. 3b). The slow loss of Alexa-488 signal from the rapidly internalized IgG suggests that intracellular antibody degradation and cellular efflux of degraded fluorophore is relatively slow and the more rapid decrease in total signal for sm3E is primarily driven by scFv dissociation or antigen shedding. The low affinity scFv ds-shMFE-M dissociates completely from the cell surface before any significant internalization takes place (data not shown).

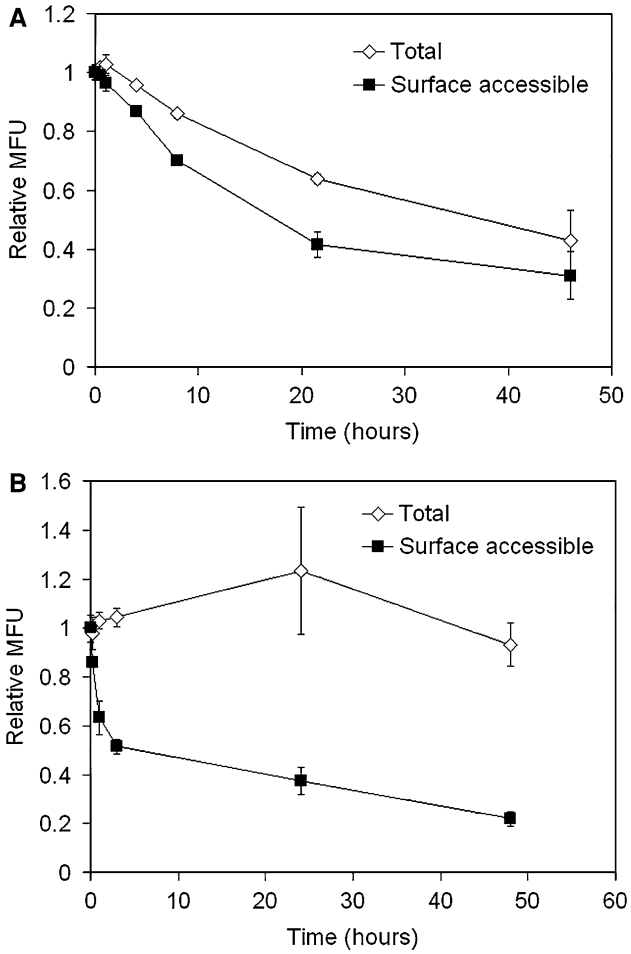

Fig. 3 Internalization limits antibody persistence on cell surface. LS174T cells were pulse labeled with Alexa-488 conjugated antibodies on ice then chased at 37°C. At each time point, cells were surface labeled with a PE conjugated secondary antibody, and the Alexa-488 signal (total cell associated antibody) and PE signal (surface antibody) measured by flow cytometry. The difference between the total and surface antibody pools represents internalized antibodies. The high affinity scFv sm3E (**a**) is slowly endocytosed from the cell surface while IgG M85151a (**b**) displays a more rapid decrease in surface antibody levels due to faster internalization

Fluorescence imaging

For further confirmation of anti-CEA antibody internalization by LS174T cells, fluorescence microscopy was used to assess the subcellular distribution of antibodies following

cellular trafficking. Following a 24 h incubation at 37°C, Alexa-488 labeled anti-CEA IgGs accumulate in intracellular compartments of LS174T cells inaccessible to a PE labeled anti-mouse secondary IgG (Fig. 4a). By contrast, at 4°C, anti-CEA IgGs remain primarily at the cell surface as seen by the extensive colocalization between the primary and secondary antibodies.

To better characterize the route of antibody internalization, fluorescence colocalization studies were performed between anti-CEA scFvs and markers of endocytic pathways. Specifically, dextran, transferrin, cholera toxin B, and LysoTracker were used as markers of early endosomes, recycling endosomes, caveolae-mediated internalization, and lysosomes, respectively. In all cases, anti-CEA scFvs internalized at 37°C for 24 h showed partial, but incomplete fluorescent colocalization with the respective marker (Fig. 4b), suggesting that CEA is internalized non-specifically through multiple pathways.

Surface CEA and antibody levels

Antibodies against EGFR and other cell surface proteins have been shown to downregulate surface levels of their target antigen following binding which may have significant effects on antibody microdistribution and pharmacodynamics [13, 15]. To determine if anti-CEA antibodies are also capable of downregulating their target antigen, LS174T cells were incubated with saturating concentrations of unlabeled antibodies or antibody fragments at 37°C and the surface CEA concentration determined at each time point by labeling the cells on ice with an Alexa-488 labeled non-competitive anti-CEA antibody. Both the monovalent and bivalent high affinity scFvs (ds-sm3E-M and ds-sm3E-D), as well as the slowly internalized IgG M111147, have no effect on the surface levels of CEA (Fig. 5a). In contrast, incubation with the rapidly internalized IgG M85151a induces a 20% decrease in surface CEA levels that is sustained to 5 h. This downregulation is not observed when the cells are incubated with a monovalent Fab fragment of the antibody suggesting that the activity is valency dependent.

Antigen concentration and the number of antibody molecules bound per cell at saturation may also influence the tumor microdistribution of antibodies [37]. To quantify these parameters, the cellular fluorescence of LS174T cells labeled with saturating concentrations of Alexa-488 labeled antibodies or antibody fragments was measured and

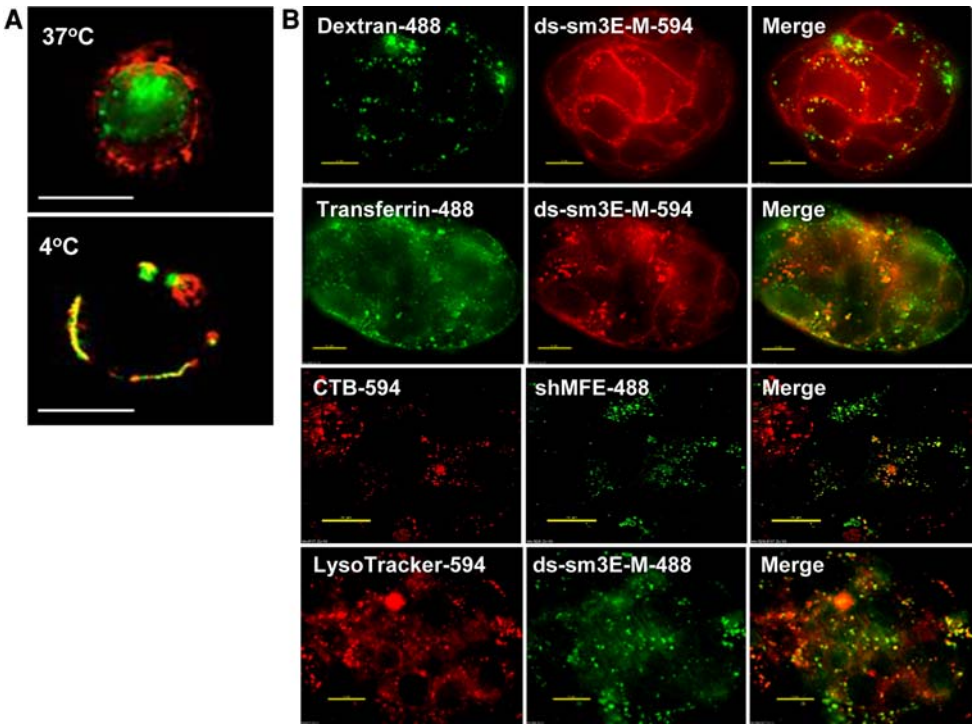

Fig. 4 Imaging anti-CEA antibody uptake. **a** Anti-CEA antibodies are trafficked into intracellular pools at 37°C. Trypsinized LS174T cells were surface labeled with Alexa-488 labeled IgG M85151a on ice and incubated for 24 h at 4°C or 37°C. Cells were then labeled with goat-anti-mouse-PE and imaged on a deconvolution microscope. When incubated at 37°C a significant fraction of the 488 labeled anti-CEA antibodies are endocytosed into an intracellular pool where they are not labeled by the secondary antibody. *Scale bar*, 20 μm. **b** Internalized anti-CEA antibodies partially colocalize with markers of endocytosis. LS174T cells were incubated overnight at 37°C with fluorescently labeled anti-CEA scFvs. Cells were then washed and incubated for 1 h with fluorescently labeled markers of endocytic and lysosomal pathways. Dual label images were taken on a deconvolution microscope. The anti-CEA scFv shows partial but incomplete colocalization with all endocytic pathway markers. Each image is a clump of 5–10 adherent LS174T cells. *Scale bar*, 10 μm

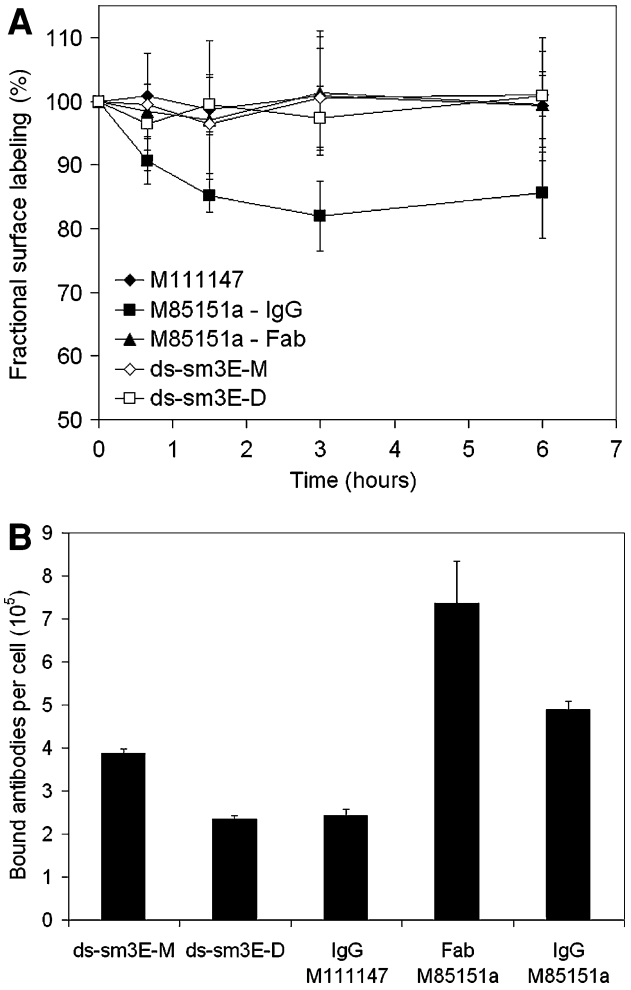

Fig. 5 Effect of antibodies on surface CEA levels. **a** IgG M85151a partially downregulates surface CEA levels. LS174T cells were incubated with unlabeled antibodies at 37°C and the relative amount of surface CEA measured at each time point by labeling with an Alexa-488 labeled non-competitive antibody. Incubation with IgG M85151a decreases surface CEA ~20%, while the other antibodies have no effect on surface CEA. All measurements done in triplicate and error bars are SD. **b** M85151a has twice as many cell bound molecules at saturation as other anti-CEA antibodies. LS174T cells were labeled to saturation with Alexa-488 conjugated antibodies and the number of molecules bound per cell calculated as described in "Materials and methods". Both the IgG and Fab versions of M85151a have approximately twice as many molecules bound at saturation as other antibodies of equivalent valency. All measurements done in triplicate and error bars are SD

converted to a number of bound molecules per cell using fluorescent calibration beads. As seen in Fig. 5b, ~400,000 molecules of the monovalent scFv ds-sm3E-M are bound to each cell at saturation, while the scFv dimer ds-sm3E-D and IgG M111147 saturate the cell with ~40% fewer molecules due to bivalent antigen binding. Interestingly, both the IgG and Fab versions of M85151a bind with approximately twice as many molecules per cell at saturation as the other antibodies of equivalent valency. The greater cell surface binding at saturation for M85151a compared to M111147 was also observed on HT-1080-CEA cells (Supplemental Fig. 2) while neither antibody binds HT-1080 in the absence of CEA expression suggesting that M85151a's higher cell labeling is mediated by interactions with CEA and is not due to binding other proteins on the cell surface. The difference in cell binding stoichiometry is also not due to heterogeneous antigen that is partially unreactive with the scFvs and M111147 since >95% of soluble CEA elutes as a complex on size exclusion chromatography when incubated with an excess of any of the tested antibodies (data not shown). One potential explanation for the twofold greater cell binding of M85151a is the possibility that this antibody binds to two different epitopes on each CEA molecule (see "Discussion").

Metabolic turnover of CEA

Finally, we examined the metabolic turnover of the target antigen CEA in the absence of antibody using a biotinylation pulse-chase assay. LS174T cells were surface biotinylated with a NHS-SS-biotin reagent, washed, and incubated at 37°C. At each time point, cells were lysed, biotinylated proteins affinity purified with streptavidin resin, and eluted samples analyzed with anti-CEA western blots. The band

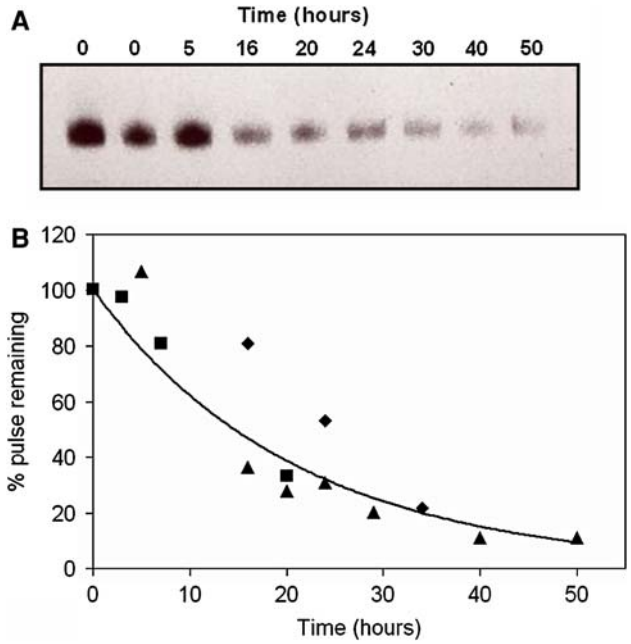

Fig. 6 Metabolic turnover of CEA. Cell surface proteins were pulsed with biotin using an NHS-SS-biotin reagent and chased at 37°C. At each time point, cells were lysed, biotinylated proteins pulled down with streptavidin resin, and the pulldown blotted for CEA as described in "Materials and methods". Band intensities were normalized to the signal at time zero and fit to a negative exponential. **a** Western blot from a single experiment. **b** Pooled data from three separate experiments fit to a negative exponential. Each symbol in (**b**) represents a different experiment. CEA is degraded with a half-time of 15 h, similar to the internalization rate of the anti-CEA antibodies

intensity of the purified samples decreases over time as biotin-pulsed CEA molecules are catabolized by the cells (Fig. 6a). Band intensities were quantified and fit to an exponential decay to derive a rate of CEA turnover (Fig. 6b). Using this assay, the half-time for CEA turnover was determined to be 15 h. This value is approximately equal to the rate of antibody internalization (Fig. 2c), suggesting that the metabolic turnover of CEA drives antibody uptake and that the antibodies themselves do little to modulate this rate—with the exception of IgG M85151a.

Discussion

Theoretical analyses of antibody transport in solid tumors suggest that cellular internalization and catabolism of bound antibodies significantly retards penetration of these drugs into the tumor. In order to test these predictions using CEA-specific antibodies as a model system, the rates of antibody and antibody fragment internalization by CEA expressing tumor cells were measured. Fluorescence measurements using flow cytometry provided a quantitative and facile method for measuring trafficking kinetics that was higher throughput than imaging approaches and avoided artifacts of incomplete antibody stripping observed with acid washing protocols.

With the exception of IgG M85151a (discussed below), all anti-CEA antibodies and antibody fragments tested were internalized in LS174T cells slowly with uptake half-times of 10–16 h. This time scale is consistent with the metabolic turnover rate of CEA in the absence of antibody ($t_{1/2} \sim 15$ h) suggesting that the antibodies are taken up passively with the antigen and do little to drive or modulate this uptake. The tested antibodies and antibody fragments have no effect on surface levels of CEA following binding, which is also consistent with a passive uptake mechanism. Since CEA is a GPI-linked protein with no cytoplasmic or transmembrane protein domains, the observed uptake is likely the result of bulk membrane turnover rather than specific protein-mediated pathways [19]. Such non-specific trafficking of CEA may explain the results of immunofluorescent microscopy experiments in which internalized anti-CEA scFvs colocalized partially but incompletely with markers of multiple endocytic pathways. Similar slow metabolic turnover has been observed for other antibodies targeting non-receptor cell surface antigens [23].

Slow cellular uptake of the high affinity anti-CEA scFv ds-sm3E-M on the order of 11–17 h was also observed in two additional colon carcinoma cell lines, LIM1215 and SW-1222. In contrast, uptake was significantly faster ($t_{1/2} \sim 4$ h) in a fibrosarcoma cell line HT-1080 transfected with a CEA expression plasmid. It is unclear if this faster uptake is due to greater overall cell surface turnover in this cell line or some function of the artificial CEA overexpression.

Cellular trafficking studies in other systems have suggested that the affinity and valency of soluble ligands or antibodies may alter cellular uptake rates by influencing the fraction of molecules that are recycled to the cell surface following endocytosis, or by altering antigen clustering dynamics on the cell surface [12, 30]. In the case of the anti-CEA scFvs examined here, however, no significant difference in the net uptake constant (k_e) was observed for molecules with a range of affinity, stability to protease digestion, and valency. The lack of an affinity dependency may suggest that CEA binding occupancy in the endosome has little effect on the fraction of antibodies that are recycled versus degraded, or alternatively, that both the high and low affinity scFvs are able to maintain antigen binding in the endosome due to the high concentration of CEA. Similarly, the equivalent uptake of the monovalent and bivalent scFvs suggests that crosslinking of two CEA molecules on the cell surface has little effect on the antigen's distribution or trafficking. This result is consistent with previous observations that bivalent binding of IgGs against folate receptor, another GPI-linked protein, were insufficient to drive receptor clustering on the surface or increase uptake [28].

Although affinity and valency have little impact on the uptake constant (k_e) of anti-CEA antibodies, they may still influence the total amount of internalized antibody which depends on both k_e and the amount of antibody bound ($d[Ab]_{internal}/dt = k_e \times [Ab]_{bound}$). This distinction is clearly observed with the behavior of the low affinity scFv ds-shMFE-M in the continuous uptake and surface decay experiments. While ds-shMFE-M is internalized when continuously incubated with the cells at a 20 nM concentration, it dissociates from the cells prior to internalization in the surface decay assay. Both of these cases are relevant to in vivo tumor targeting. The continuous uptake experiments are similar to the loading phase of tumor targeting where a high plasma concentration maintains a sufficient antibody concentration in the tumor to drive binding and internalization, while the surface decay assay represents the retention phase when antibody clears from the plasma and tumor. In contrast to the low affinity case, the high affinity and bivalent antibodies have dissociation rates (k_{off}) slower than the internalization rate (k_e) such that binding will be essentially irreversible in both targeting regimes [23].

Unlike the remainder of the tested antibodies, IgG M85151a exhibited a distinct trafficking profile with a significantly faster net uptake rate ($t_{1/2} \sim 5$ h) and the ability to downregulate surface CEA. These properties were both valency dependent, as a monovalent Fab fragment of M85151a was internalized slowly and had no effect on surface CEA. Both the M85151a IgG and Fab also bind with

approximately twice as many molecules per cell at saturation as compared to other antibodies of equivalent valency. One potential explanation for this twofold higher cell binding stoichiometry is the possibility that these antibodies bind to more than one epitope per CEA molecule. Monoclonal antibodies capable of binding multiple epitopes per CEA molecule have been reported previously, a phenonmenon attributed to the high sequence homology of repeat domains within the antigen [20, 29, 40]. If M85151a does in fact bind two epitopes per CEA molecule, it may also provide a mechanism for the faster uptake. Bivalent antibodies that bind to a single epitope per antigen can only crosslink two molecules. In contrast, a bivalent molecule that binds more than one epitope per molecule may be able to crosslink larger clusters of antigens. Previous studies have demonstrated that the formation of large clusters of GPI-linked proteins can increase antigen localization in caveolae, as well as drive greater antigen internalization and downregulation [10, 15, 28].

Although the experiments presented here indicate that the internalization of anti-CEA antibodies and antibody fragments in LS174T cells occurs slowly, this rate is sufficient to significantly impact antibody distribution and retention in the tumor. Thurber and Wittrup have shown that anti-CEA scFvs are able to penetrate significantly farther into LS174T spheroids when incubated at 20°C versus 37°C due to reduced cellular internalization [36]. Similarly, Ackermann et al. have demonstrated that the slowly internalized IgG M111147 is able to penetrate significantly farther into LS174T spheroids than the rapidly internalized IgG M85151a (in preparation). The difference in penetration distance can be quantitatively predicted from the k_e values and cell surface binding stoichiometry measured here.

Based on these results and other computational predictions, we suggest that antibodies with slow cellular internalization rates should have advantages for most tumor targeting applications due to their improved penetration and retention in the tumor (with the exception of immunotoxins and antibody-drugs that must be internalized to be cytotoxic [39]). In some cases, it may be possible to engineer more slowly internalized antibodies by either selecting for proteins that are efficiently recycled following endocytosis or by using monovalent antibodies that avoid faster uptake due to antigen clustering. Alternatively, antibody internalization may be reduced by targeting antigens with slower metabolic turnover. One promising target is the colorectal cancer marker A33 which has extended cell surface persistence due to interactions at the tight junction [1].

Acknowledgments This work was supported by CA101830 and the NIGMS/MIT Biotechnology Training Program. The authors also thank the Ludwig Institute and Dr. Gerald Prud'homme for cell lines and plasmids.

References

1. Ackerman M, Chalouni C, Raman V, Schmidt M, Ritter G, Mellman I, Wittrup KD (2008) A33 antigen displays persistent surface expression. Cancer Immunol Immunother (in press)
2. Adams GP et al (2001) High affinity restricts the localization and tumor penetration of single-chain fv antibody molecules. Cancer Res 61:4750–4755
3. Adams GP, Weiner LM (2005) Monoclonal antibody therapy of cancer. Nat Biotechnol 23:1147–1157
4. Austin CD et al (2004) Endocytosis and sorting of ErbB2 and the site of action of cancer therapeutics trastuzumab and geldanamycin. Mol Biol Cell 15:5268–5282
5. Baxter LT, Jain RK (1991) Transport of fluid and macromolecules in tumors. III. Role of binding and metabolism. Microvasc Res 41:5–23
6. Beckman RA, Weiner LM, Davis HM (2007) Antibody constructs in cancer therapy: protein engineering strategies to improve exposure in solid tumors. Cancer 109:170–179
7. Behr TM et al (2000) Therapeutic advantages of Auger electron-over beta-emitting radiometals or radioiodine when conjugated to internalizing antibodies. Eur J Nucl Med 27:753–765
8. Bryan JN et al (2005) Comparative uptakes and biodistributions of internalizing versus noninternalizing copper-64 radioimmunoconjugates in cell and animal models of colon cancer. Nucl Med Biol 32:851–858
9. Cai W et al (2007) PET imaging of colorectal cancer in xenograft-bearing mice by use of an 18F-labeled T84.66 anti-carcinoembryonic antigen diabody. J Nucl Med 48:304–310
10. Casalini P et al (1997) Tumor pretargeting: role of avidin/streptavidin on monoclonal antibody internalization. J Nucl Med 38:1378–1381
11. Dooley H et al (1998) Stabilization of antibody fragments in adverse environments. Biotechnol Appl Biochem 28(Pt 1):77–83
12. Fallon EM, Lauffenburger DA (2000) Computational model for effects of ligand/receptor binding properties on interleukin-2 trafficking dynamics and T cell proliferation response. Biotechnol Prog 16:905–916
13. Fan Z et al (1994) Antibody-induced epidermal growth factor receptor dimerization mediates inhibition of autocrine proliferation of A431 squamous carcinoma cells. J Biol Chem 269:27595–27602
14. Ford CH et al (1996) Novel flow cytometric analysis of the progress and route of internalization of a monoclonal anti-carcinoembryonic antigen (CEA) antibody. Cytometry 23:228–240
15. Friedman LM et al (2005) Synergistic down-regulation of receptor tyrosine kinases by combinations of mAbs: implications for cancer immunotherapy. Proc Natl Acad Sci USA 102:1915–1920
16. Fujimori K et al (1990) A modeling analysis of monoclonal antibody percolation through tumors: a binding-site barrier. J Nucl Med 31:1191–1198
17. Graff CP et al (2004) Directed evolution of an anti-carcinoembryonic antigen scFv with a 4-day monovalent dissociation half-time at 37 °C. Protein Eng Des Sel 17:293–304
18. Graff CP, Wittrup KD (2003) Theoretical analysis of antibody targeting of tumor spheroids: importance of dosage for penetration, and affinity for retention. Cancer Res 63:1288–1296
19. Hammarstrom S (1999) The carcinoembryonic antigen (CEA) family: structures, suggested functions and expression in normal and malignant tissues. Semin Cancer Biol 9:67–81
20. Hedin A, Hammarstrom S, Larsson A (1982) Specificities and binding properties of eight monoclonal antibodies against carcinoembryonic antigen. Mol Immunol 19:1641–1648
21. Jain RK (2001) Delivery of molecular and cellular medicine to solid tumors. Adv Drug Deliv Rev 46:149–168

22. Kraeber-Bodere F et al (2006) Targeting, toxicity, and efficacy of 2-Step, pretargeted radioimmunotherapy using a chimeric bispecific antibody and 131I-labeled bivalent hapten in a phase I optimization clinical trial. J Nucl Med 47:247–255
23. Kyriakos RJ et al (1992) The fate of antibodies bound to the surface of tumor cells in vitro. Cancer Res 52:835–842
24. Lee YC et al (2002) Reversible dimer formation and stability of the anti-tumour single-chain Fv antibody MFE-23 by neutron scattering, analytical ultracentrifugation, and NMR and FT-IR spectroscopy. J Mol Biol 320:107–127
25. Liu G et al (2005) Further investigations of morpholino pretargeting in mice–establishing quantitative relations in tumor. Eur J Nucl Med Mol Imaging 32:1115–1123
26. Lund KA et al (1990) Quantitative analysis of the endocytic system involved in hormone-induced receptor internalization. J Biol Chem 265:15713–15723
27. Mattes MJ (2005) Binding parameters of antibodies: pseudo-affinity and other misconceptions. Cancer Immunol Immunother 54:513–516
28. Mayor S, Rothberg KG, Maxfield FR (1994) Sequestration of GPI-anchored proteins in caveolae triggered by cross-linking. Science 264:1948–1951
29. Paxton RJ et al (1987) Sequence analysis of carcinoembryonic antigen: identification of glycosylation sites and homology with the immunoglobulin supergene family. Proc Natl Acad Sci USA 84:920–924
30. Rao BM, Lauffenburger DA, Wittrup KD (2005) Integrating cell-level kinetic modeling into the design of engineered protein therapeutics. Nat Biotechnol 23:191–194
31. Reiter Y et al (1996) Engineering antibody Fv fragments for cancer detection and therapy: disulfide-stabilized Fv fragments. Nat Biotechnol 14:1239–1245
32. Sharma SK et al (2005) Sustained tumor regression of human colorectal cancer xenografts using a multifunctional mannosylated fusion protein in antibody-directed enzyme prodrug therapy. Clin Cancer Res 11:814–825
33. Shih LB et al (1994) Internalization of an intact doxorubicin immunoconjugate. Cancer Immunol Immunother 38:92–98
34. Stein R et al (1999) Carcinoembryonic antigen as a target for radioimmunotherapy of human medullary thyroid carcinoma: antibody processing, targeting, and experimental therapy with 131I and 90Y labeled MAbs. Cancer Biother Radiopharm 14:37–47
35. Sung C, van Osdol WW (1995) Pharmacokinetic comparison of direct antibody targeting with pretargeting protocols based on streptavidin–biotin binding. J Nucl Med 36:867–876
36. Thurber G, Wittrup KD (2008) Quantitative spatiotemporal analysis of antibody diffusion and endocytic consumption in tumor spheroids. Cancer Res (in press)
37. Thurber G, Zajik SC, Wittrup KD (2007) Theoretical criteria for antibody saturation of tumors and micrometastases. J Nucl Med 48:995–999
38. Wegener WA et al (2000) Safety and efficacy of arcitumomab imaging in colorectal cancer after repeated administration. J Nucl Med 41:1016–1020
39. Yazdi PT, Wenning LA, Murphy RM (1995) Influence of cellular trafficking on protein synthesis inhibition of immunotoxins directed against the transferrin receptor. Cancer Res 55:3763–3771
40. Zimmermann W et al (1987) Isolation and characterization of cDNA clones encoding the human carcinoembryonic antigen reveal a highly conserved repeating structure. Proc Natl Acad Sci USA 84:2960–2964